Journal of proteome research

pubs.acs.org/jpr

Article

High-Throughput Salivary Metabolite Profiling on an Ultralow Noise Tip-Enhanced Laser Desorption Ionization Mass Spectrometry Platform for Noninvasive Diagnosis of Early Lung Cancer

Xinrong Jiang, Xiaoming Chen, Zhao Chen, Jiekai Yu, Haizhou Lou,* and Jianmin Wu*

Cite This: *J. Proteome Res.* 2021, 20, 4346−4356

Read Online

ACCESS | Metrics & More | Article Recommendations | Supporting Information

ABSTRACT: Lung cancer (LC) is a widespread cancer that is the cause of the highest mortality rate accounting for 25% of all cancer deaths. To date, most LC patients are diagnosed at the advanced stage owing to the lack of obvious symptoms in the early stage and the limitations of current clinical diagnostic techniques. Therefore, developing a high throughput technique for early screening is of great importance. In this work, we established an effective and rapid salivary metabolic analysis platform for early LC diagnosis and combined metabolomics and transcriptomics to reveal the metabolic fluctuations correlated to LC. Saliva samples were collected from a total of 150 volunteers including 89 patients with early LC, 11 patients with advanced LC, and 50 healthy controls. The metabolic profiling of noninvasive samples was investigated on an ultralow noise TELDI-MS platform. In addition, data normalization methods were screened and assessed to overcome the MS signal variation caused by individual difference for biomarker mining. For untargeted metabolic profiling of saliva samples, around 264 peaks could be reliably detected in each sample. After multivariate analysis, 23 metabolites were sorted out and verified to be related to the dysfunction of the amino acid and nucleotide metabolism in early LC. Notably, transcriptomic data from online TCGA repository were utilized to support findings from the salivary metabolomics experiment, including the disorder of amino acid biosynthesis and amino acid metabolism. Based on the verified differential metabolites, early LC patients could be clearly distinguished from healthy controls with a sensitivity of 97.2% and a specificity of 92%. The ultralow noise TELDI-MS platform displayed satisfactory ability to explore salivary metabolite information and discover potential biomarkers that may help develop a noninvasive screening tool for early LC.

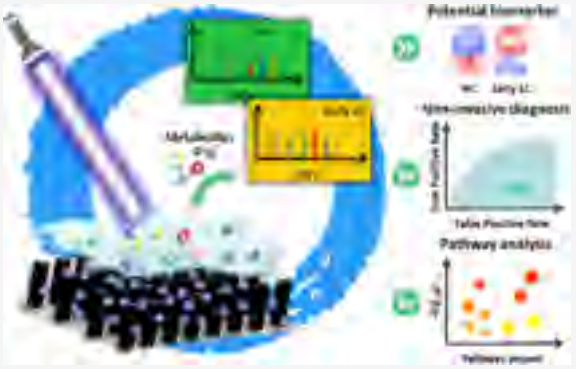

KEYWORDS: *salivary metabolomics, lung cancer, high-throughput, noninvasive diagnosis*

INTRODUCTION

Lung cancer (LC), one of the most prevalent types of cancer in the world, is the cause of the highest mortality rate accounting for 25% of all cancer deaths. The 5-year survival rate for LC patients diagnosed at advanced stages is less than 15%, while for those diagnosed at early stages, the survival rate can reach 70−80%, which highlights the importance of early diagnosis to improve the overall survival.[1] However, early screening of LC remains a challenge due to the lack of obvious symptoms and the limitations of current clinical diagnostic techniques.[2,3] The gold standard for tumor diagnosis is histopathology, which is unsuitable for screening due to the invasive sampling procedure. Currently, low-dose CT has become the first choice for noninvasively screening LC in population because of its high sensitivity, but its application has been hampered by the low sensitivity among those who have never smoked, low specificity (high false-positive rate), and high cost.[4] Therefore, rapid and effective techniques for the early screening of LC in population with high sensitivity and specificity are in urgent need.

Saliva is a noninvasive biological fluid containing trace metals, metabolites, proteins, lipids, nucleic acid, and so forth.[5] It has been confirmed that molecular changes in saliva can reflect human diseases.[6−8] Compared with commonly used clinical samples like serum and tissue samples, the collection process of saliva samples is noninvasive, less harmful, and more accessible. Accordingly, saliva may become a promising biological fluid for disease screening and health monitoring in large population. Metabolomics is a new discipline following genomics and proteomics. By monitoring metabolite differences in biological fluids or tissues, biomarkers for disease screening, early warning, and classification can be discovered.[9]

Received: April 15, 2021
Published: August 3, 2021

Table 1. Clinical Characteristics of the Subjects in This Study

characteristics	discovery set		validation set		advanced LC
	HC	early LC	HC	early LC	
cases	25	45	25	44	11
men, *n* (%)	10 (40.0)	16 (35.6)	9 (36.0)	15 (32.8)	7 (63.6)
age (median/range)	52.9 (12.3)	57.8 (13.4)	57.3 (15.8)	55.3 (10.9)	70.2 (6.9)
pathological diagnosis		LUAD (n = 43), SCC (n = 2)		LUAD (n = 41), SCLC (n = 1), LCC (n = 2)	LUAD (n = 7), SCC (n = 2), SCLC (n = 1), LDLC (n = 1)
stage		I (n = 45)		I (n = 44)	III (n = 1), IV (n = 10)
TNM		T1N0M0 (n = 45)		T1N0M0 (n = 44)	T4N0M1 (n = 4), T2N0M1 (n = 2), T2N2M1 (n = 2), T1N0M1 (n = 1), T2N2M0 (n = 1), T3N0M1 (n = 1)
primary/secondary		primary (n = 45)		primary (n = 43), secondary (n = 1)	primary (n = 11)
tumor size		0−1 cm (n = 23), 1−2 cm (n = 13), 2−3 cm (n = 9)		0−1 cm (n = 23), 1−2 cm (n = 12), 2−3 cm (n = 9)	2−3 cm (n = 1), 3−5 cm (n = 5), 5−7 cm (n = 1), >7 cm (n = 4)
body mass index (kg/m^2, median/range)	23.72 (3.44)	22.46 (3.41)	23.59 (2.58)	23.34 (2.96)	21.46 (3.26)
smoking habit	smokers (n = 5, 20%)	smokers (n = 13, 28%)	smokers (n = 4, 16%)	smokers (n = 11, 25%)	smokers (n = 6, 55%)
drinking habit	drinkers (n = 7, 28%)	drinkers (n = 14, 31%)	drinkers (n = 5, 20%)	drinkers (n = 13, 30%)	drinkers (n = 7, 63%)
drug usage		none		none	none

Recently, several works on LC metabolomics to search potential biomarkers in human tissues and biofluids have been reported.[10−15] The rise of metabolomics provided new insights for LC diagnosis.

The principal techniques used for salivary metabolomics include nuclear magnetic resonance (NMR) spectroscopy, gas chromatography−mass spectrometry (GC−MS), and liquid chromatography−mass spectrometry (LC−MS).[7,8,16] However, GC−MS and LC−MS required a long time for chromatographic separation, whereas NMR is less sensitive compared with MS techniques. These shortcomings may limit the application of these techniques for large-scale disease screening in population. Matrix-assisted laser desorption/ionization mass spectrometry (MALDI-MS) has been applied in the profiling of biological samples with acceptable selectivity and high throughput, which provides the possibility in large-scale clinical diagnosis.[17] Nevertheless, the platform could be severely suffered from the matrix interference in the low-molecular weight (LMW) region, especially for the metabolite with a molecular weight below 400 Da.[18,19] Our previous work has developed a tip-enhanced laser desorption/ionization (TELDI) platform using fluorinated ethylene propylene polymer (FEP)-coated vertical silicon nanowire (VSiNW) arrays. The platform displayed a high sensitivity and ultralow noise in LMW region.[20,21] With the ultralow noise TELDI-MS platform, salivary metabolites could be sensitively and reliably profiled in a high throughput way.[20]

Another challenge in the salivary metabolic analysis is the variation in secretion volume caused by different water consumptions and other physiological and pathophysiological factors, which inversely affects metabolite concentration.[22] Metabolic data without suitable normalization cannot reflect the underlying phenotype.[23] Accordingly, it is necessary to perform proper data normalization prior to statistical analysis between participant groups.

In this study, saliva samples from patients diagnosed with early LC and healthy volunteers were collected and non-targeted salivary metabolomics was investigated using an ultralow noise TELDI-MS platform. After acquiring MS spectra data, a total of six different normalization techniques were compared and screened for eliminating the external interference for salivary metabolomics such as water intake. We screened early LC-related differential metabolites in saliva samples and then performed pathway-based enrichment analysis based on these dysregulated metabolites. Besides, RNASeq data from 35 pairs of LC tissues and adjacent tissues were obtained and analyzed to verify the significantly altered metabolic pathways. Furthermore, 23 identified significant metabolites were defined as potential biomarker candidates for early LC and further selected for discriminant analysis. Based on the selected feature metabolites, orthogonal projections to latent structures discriminant analysis (OPLS-DA), principal component analysis (PCA), and cluster analysis can successfully discriminate early LC from normal control and advanced LC. The artificial neural network (ANN) model indicated that the group of early LC patients can be discriminated from the healthy group with a sensitivity of 97.2% and specificity of 92% using the panel of feature metabolites.

MATERIALS AND METHODS

Materials and Reagents

Single-crystal silicon wafers (p type, ⟨100⟩, 5−10 Ω·cm) were purchased from Lijing Silicon Materials Co. (Quzhou, China). Hydrofluoric acid (HF, 40%) and ethanol (EtOH) were purchased from Sinopharm Chemical Reagent Co. (Shanghai, China). Silver nitrate ($AgNO_3$), aspartic acid, glutamine, histidine, glutamic acid, proline, γ-aminobutyric acid, serine, cytosine, uracil, creatinine, valine, pyroglutamic acid, ketoleucine, adenine, imidazolepropionic acid, allysine, phenylglyoxylic acid, guanine, xanthine, 3-hydroxyanthranilic acid, gentisic acid, *N*-acetylproline, arginine, *N*-acetyltaurine, *N*-acetyl-L-glutamic acid, *N*-acetylhistidine, and glycyl-phenylalanine standards were purchased from Aladdin Co. (Shanghai, China). FEP preparation was purchased from Jinhua Yonghe Fluorochemical Co. (Jinhua, China).

https://doi.org/10.1021/acs.jproteome.1c00310
J. Proteome Res. 2021, 20, 4346−4356

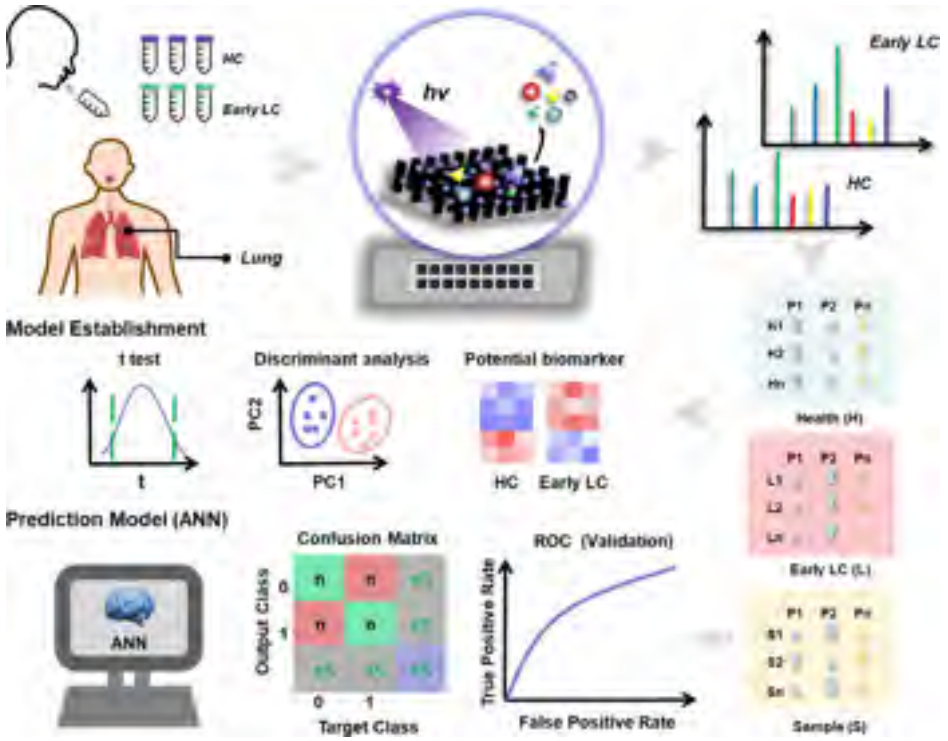

Figure 1. Workflow of metabolic analysis of saliva samples from the early LC group and controls and establishment of the prediction model for early LC diagnosis.

Ultralow Noise TELDI Substrate Fabrication

The detailed fabrication procedure of FEP@VSiNWs has been described in our previous work.[20] Briefly, silicon wafer was cut to 3 cm × 3 cm chips and then immersed in 0.02 M $AgNO_3$ and 4.8 M HF mixed solution. After etching for 15 min, the excess Ag catalyst was dissolved with dilute nitric acid (HNO_3, 1:1 v/v). For initiator loading, 100 μL of FEP preparation was applied onto the surface of the freshly etched chip. After 30 min, the excess initiator was removed on a spin coater to obtain a uniform surface.

Collection and Pretreatment of Saliva Samples

Totally, 50 healthy volunteers and 100 LC patients (89 patients with early LC and 11 patients with advanced LC) participated in the saliva collection project. The detailed demographic information of participants is provided in Table 1. The saliva collection was implemented in Sir Run Run Shaw Hospital of Zhejiang University between 8:30 and 10:30 am. Before collection, all individuals were refrained from eating, drinking, or smoking for at least 2 h. The detailed procedure of saliva collection and preparation is described in the Supporting Information. After removing insoluble residues and precipitating proteins in saliva, the final supernatant was diluted with ultrapure water (1:4 v/v) and stored in the refrigerator at −80 °C until use. The Ethical Committee of the Sir Run Run Shaw Hospital of Zhejiang University approved the protocol (no. 20201028-39), and the methods were carried out in accordance with the approved guidelines.

Salivary Metabolite Profiling on the TELDI-MS Platform

The workflow of metabolic analysis of saliva samples is shown in Figure 1. Prior to MS measurement, saliva samples were thawed at 4 °C, the prepared FEP@VSiNWs substrate was cut into 4 mm × 4 mm chips, and then, a 2 μL droplet of each sample was deposited onto one chip, which was stuck onto a custom-made plate with a carbon conductive adhesive tape. Each custom-made plate can load 48 chips, and two plates can be simultaneously inserted into the instrument for each test. After drying, plates were inserted into the ultrafleXtreme MALDI-tandem time-of-flight (TOF/TOF) instrument (Bruker Daltonics Co.) equipped with a 355 nm Nd:YAG laser beam. Mass spectra were obtained under the reflecting negative-ion mode at the m/z range of 20−350 Da. The voltages of ion source 1 and ion source 2 were set at 20.00 and 17.75 kV, the lens was set at 8.50 kV, and the reflector 1 and reflector 2 were set at 21.10 and 10.70 kV, respectively. The pulsed ion extraction was set at 120 ns, and the laser parameter was set at 4_large. For each spectrum, laser shots were added 2000 times. All measurements were repeatedly performed three times.

Data Normalization Methods Applied to Saliva

A total of six different normalization techniques were investigated to eliminate extraneous factors-to-sample variation and reduce the variation within each metabolite. In detail, the data-driven techniques used here were normalization to intensity of the highest peak signal (HSN), normalization to MS "total useful signal", linear baseline normalization, cyclic loess normalization, probabilistic quotient normalization, and cubic spline normalization. The last four normalization methods were implemented in the statistical computing language R using R 3.5.2 software.[24] The detailed R code is provided in the Supporting Information.

Data Handling and Statistical Analysis

The workflow of the statistical analysis of saliva samples is presented in Figure S1. FlexAnalysis (Bruker Daltonics Co.) was utilized for mass spectra acquisition and processing. The selection of feature peaks (S/N > 3) was completed by ClinproTools software (Bruker Daltonics Co.), and then, a list

https://doi.org/10.1021/acs.jproteome.1c00310
J. Proteome Res. 2021, 20, 4346−4356

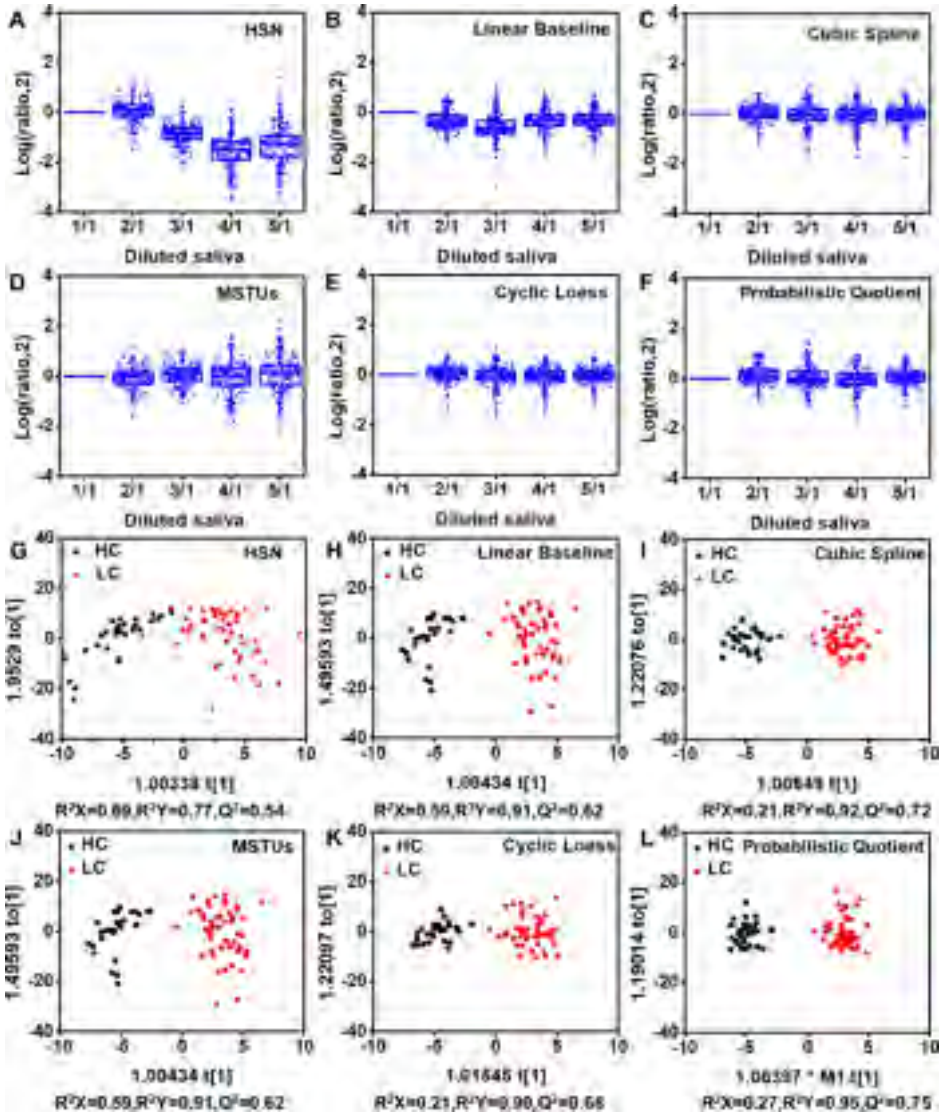

Figure 2. (A–F) Peak ratio distributions of diluted saliva samples (1S, 0.75S, 0.5S, 0.25S, and 0.125S) presented using box plots after six normalization methods. 1, 2, 3, 4, and 5 represent 1S, 0.75S, 0.5S, 0.25S, and 0.125S samples, respectively. The MS peaks detected in each sample were compared with the original 1S sample. (G–L) Score plot for the OPLS-DA model built with the normalized data set; saliva samples collected from 30 healthy controls and 30 early LC patients were utilized for the evaluation of discrimination results after six normalization techniques.

of peaks were provided. After normalization, Student's *t*-test was performed using MATLAB software. Then, PCA and cluster analysis were performed by MATLAB, and OPLS-DA was completed by SIMCA software. Also, an ANN model with a multilayer perception structure was built in MATLAB software based on the peak data set of differential metabolites. In the ANN model, early LC patients were set as positive, while healthy volunteers were set as negative parts. The training set occupied 70% of the data set, while 15% data were used as the validation set and the other 15% data were set as the testing set for evaluation of prediction accuracy. The data set was composed of the averaged data of three replicates on each saliva sample. The built model was then verified by the validation set to obtain the sensitivity, specificity, and AUC values. The impact pathway of early LC-related metabolites was analyzed based on MetaboAnalyst.

Salivary Differential Metabolite Identification

MALDI-TOF/TOF MS/MS (tandem MS) and UPLC–MS/MS were combined to identify the differential metabolites in saliva samples. UPLC–MS/MS analysis of saliva samples provided the exact molecular weights and main fragment peaks, which were utilized to identify potential metabolic biomarkers by searching the Human Metabolome Database (http://www.hmdb.ca/). The identified metabolites were further verified by purchased standard reagents through comparing the exact mass and fragment profile obtained from saliva samples and standard samples on MALDI-TOF/TOF MS/MS. Detailed experimental parameters of UPLC–MS analysis are provided in the Supporting Information.

RNA-Seq Analysis

The transcriptomics profiles of 35 LC tissues and 35 adjacent tissues were obtained from the TCGA database (https://cancergenome.nih.gov). To discover the changes in gene pathways related to metabolism, statistical analysis was performed using R 3.5.2 software. The differentially expressed genes between indicated groups were screened out by the R edgeR package. The false discovery rate (FDR) value is calculated by the R function *p*.adjust based on the Benjamini–

https://doi.org/10.1021/acs.jproteome.1c00310
J. Proteome Res. 2021, 20, 4346–4356

Hochberg method, which can well control the false positive rate and maintain the statistical detection power. Statistical significance was defined as FDR < 0.05 and $|\log_2 FC| > 1$. Gene ontology and KEGG pathway enrichment analysis were performed by the DAVID database (https://david.ncifcrf.gov/), and the heatmap of significant genes was made by the R pheatmap package.

RESULTS AND DISCUSSION

Salivary Metabolic Profiling

The collected saliva cases (50 healthy controls [HC], 89 early LC, and 11 advanced LC) were divided into two batches for TELDI-MS data acquisition (Table 1). From the first batch of saliva samples, 264 common peaks ($S/N > 3$) were observed and further selected to characterize the repeatability of the TELDI-MS platform in saliva detection. As shown in Figure S2, MS spectra obtained from three groups appear significantly different in the metabolic fingerprint region. This initial work demonstrated that metabolic profiles acquired by TELDI-MS contain underlying bioinformation that can differentiate HC, early LC, and advanced LC.

Screening Normalization Methods for Salivary Metabolic Analysis

Saliva is distinguished from many other biofluids used in metabolomics studies because of the variation in solute concentration affected by secreted volume. Therefore, proper normalization is required to minimize the impact of external factors such as water consumption on downstream analysis. Currently, various normalization techniques such as creatinine ratio, osmolality, and specific gravity are used to account for the renal dilution, as urine samples face the same challenge in metabolic analysis.[25,26] However, creatinine-based corrections are influenced by multiple factors such as age, race, physical activity, and gender.[27] The accuracy of osmolality measurements is affected by insoluble particles and sample heterogeneity.[28] Normalization of metabolic data using specific gravity would be problematic in the presence of large molecules because specific gravity normalization is strongly influenced by both the number of particles in the solution and their size.[26] Moreover, considering the practical application in clinical screening, the data-driven normalization method seems to be a better option for normalizing data sets from large-scale experiments.[24]

In this study, six kinds of data-driven normalization methods were screened to eliminate extraneous factors-to-sample variation and reduce the variation within each metabolite. In-batch and interbatch stability was presented in box plots by calculating the peak ratios of replicated measurements after normalization. Because there are few biological and physical variations between replicated measurements, the log ratios should be close to 0. Compared with other methods, HSN results in worse stability in the variation of replicated experiments (Figures S3 and S4). Besides, the correction effect of different normalization methods on saliva dilution was expressed as normalized peak ratios between diluted saliva samples and the original 1S sample. As shown in Figure 2A−F, cyclic loess, cubic spline, and probabilistic quotient normalization produced relatively stable and reliable normalized peak data during the dilution process. To statistically describe the fluctuation of each normalized metabolic peak within the same group, we calculated the peak ratios of each metabolite to the group average value in 10 individual saliva samples. As shown in Figures S5 and S6, there was little variation within each metabolite after cyclic loess, cubic spline, and probabilistic quotient normalization, no matter whether in the healthy or early LC group. To evaluate the discrimination results of different normalization methods, data acquired from 30 healthy volunteers and 30 patients diagnosed with early LC were normalized before importing into OPLS-DA analysis. In theory, the closer the R^2Y and Q^2 values are to 1, the more credible the built model is. As shown in Figure 2G−L, probabilistic quotient normalization provided the best discrimination result with $R^2Y = 0.95$ and $Q^2 = 0.75$. Based on all the abovementioned descriptions, the probabilistic quotient normalization method was chosen for subsequent salivary metabolic analysis.

Discovery and Validation of Abnormal Metabolic Signatures in Early LC

To discover the differential metabolites in early LC patients, Student's *t*-test was performed. FDR correction was further completed based on the Benjamini−Hochberg method. In this study, metabolic feature peaks with VIP > 1, $p < 0.05$, and $q < 0.05$ were defined as significantly differential biomarker candidates. Finally, a total of 24 metabolites were sorted out, which were further verified using the validation cohort, including 25 healthy volunteers and 44 patients diagnosed with early LC. Among them, 23 metabolites were verified to be significantly differential in both cohorts and the same change trends of these biomarker candidates were observed in the validation set (Table S1). The detailed identification information of the verified metabolic biomarker candidates is described in Tables S2 and S3, and the representative mass spectra of saliva samples collected from two groups in the metabolic fingerprint region are presented in Figure S7 (Supporting Information). Compared with the HC group, GABA, cytosine, uracil, creatinine, pyroglutamic acid, ketoleucine, adenine, imidazolepropionic acid, allysine, guanine, 3-hydroxyanthranilic acid, gentisic acid, *N*-acetylproline, and *N*-acetylhistidine were upregulated in early LC patients, whereas serine, proline, valine, phenylglyoxylic acid, xanthine, arginine, *N*-acetyl-L-glutamic acid, *N*-acetyltaurine, and glycyl-phenylalanine were downregulated. The downregulation of amino acids including serine, arginine, valine, and proline and the upregulation of downstream metabolites of amino acid metabolism including ketoleucine, *N*-acetylhistidine, imidazolepropionic acid, *N*-acetylproline, allysine, gentisic acid, 3-hydroxyanthranilic acid, γ-aminobutyric acid, and pyroglutamic acid were observed in the early LC group, which were consistent with previous studies on LC.[10,11,14,29−31] This may be a consequence of protein malnutrition and the increase of amino acid demand caused by tumor growth.[10] Besides, several compounds associated with purine and pyrimidine biosynthesis were significantly increased in the early LC group compared with healthy controls, including guanine, adenine, cytosine, and uracil.[32,33] The decreased levels of xanthine were assumed to correspond to the disorder of purine metabolism, which has been confirmed in numerous earlier studies on LC.[14] In the present study, creatinine levels were significantly higher in early LC patients than in controls, which has been observed in urine samples.[34] In the human body, creatine is synthesized from methionine, glycine, and arginine and further reacts to produce creatinine. Therefore, the increase in creatinine levels may be related to the upregulated amino acid metabolism. Glycyl-phenylalanine is an incomplete breakdown product of

https://doi.org/10.1021/acs.jproteome.1c00310
J. Proteome Res. 2021, 20, 4346−4356

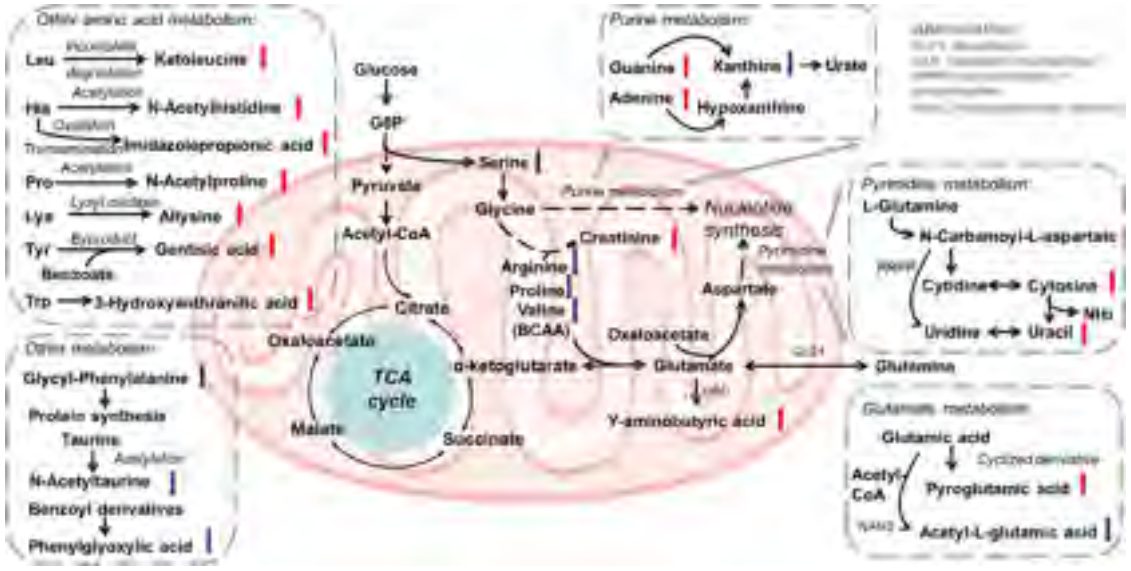

Figure 3. Pathway map of the differential metabolites in early LC. The blue and red arrows represent the downregulation and upregulation of metabolites in early LC, respectively.

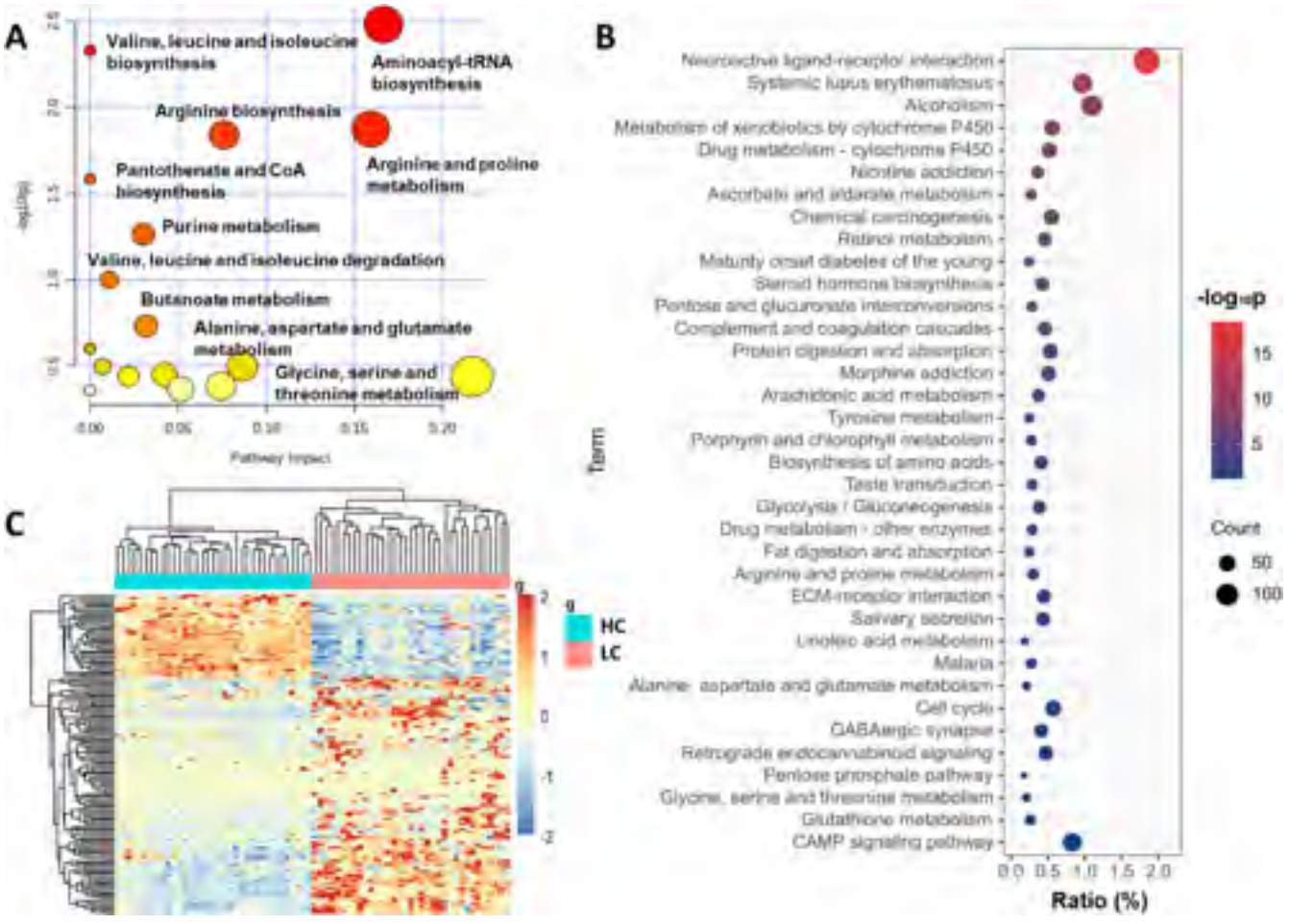

Figure 4. Globally disturbed metabolic pathways in the LC group. (A) Impact pathway analysis of early LC-related differential metabolites based on MetaboAnalyst. The significance of the metabolic disorder was presented in the circle size and color depth. (B) KEGG pathway enrichment analysis of differential genes extracted from LC tissues and adjacent normal tissues. (C) Heatmap analysis of significant genes in two groups. Significant genes used here are evolved in the related metabolic pathway, including protein digestion and absorption, biosynthesis of amino acid, salivary secretion, arginine and proline metabolism, alanine/aspartate/glutamate metabolism, glycine/serine/threonine metabolism.

https://doi.org/10.1021/acs.jproteome.1c00310
J. Proteome Res. 2021, 20, 4346−4356

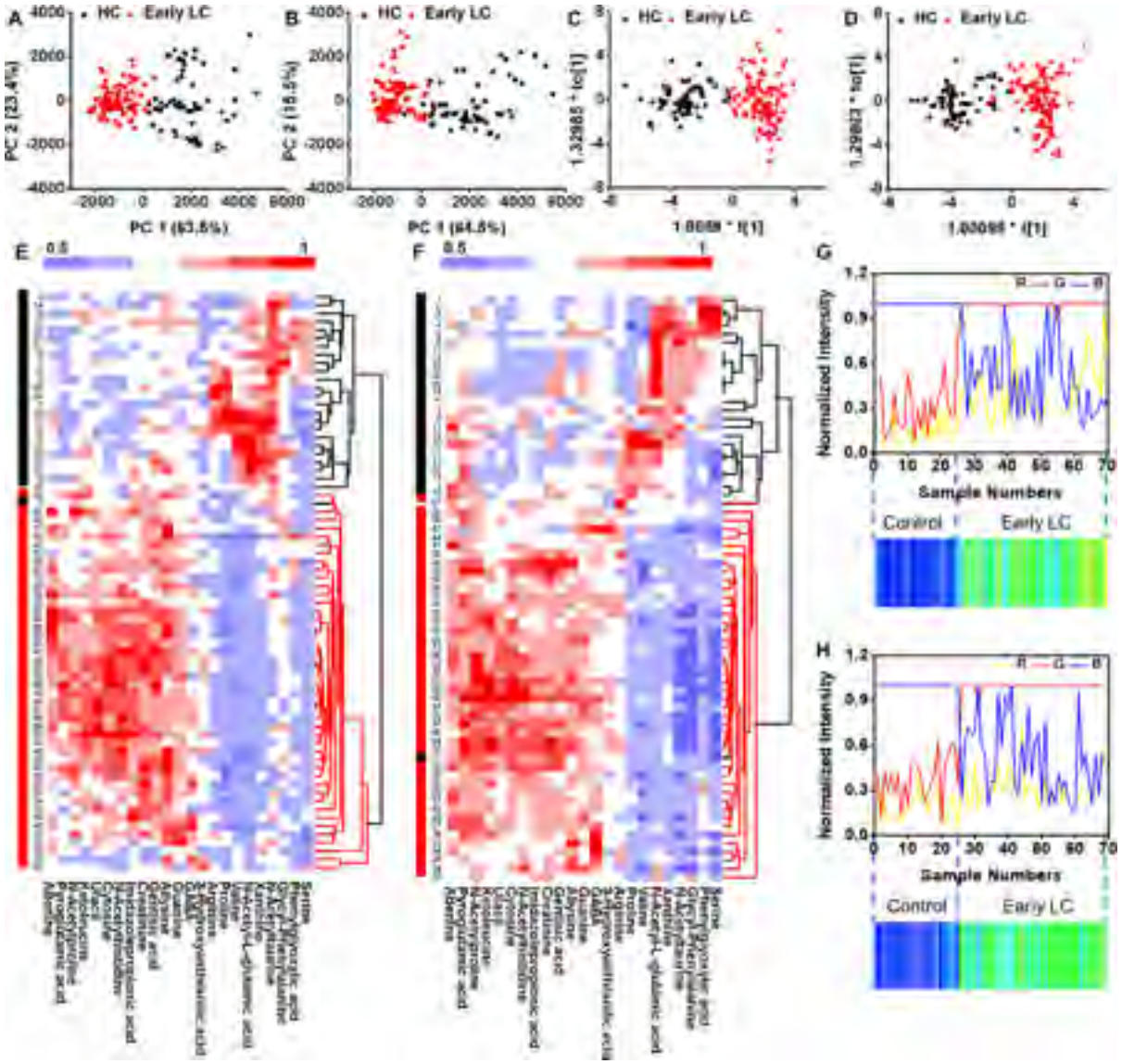

Figure 5. Multivariate analysis for discrimination between early LC patients and control individuals. (A,B) Score plots for the PCA model built with the normalized intensities of 23 selected metabolites in the discovery and validation sets, respectively. (C,D) OPLS-DA results based on the potential biomarkers. (C) In the discovery set, explained variance $R^2Y = 0.848$ and predicted variance $Q^2 = 0.81$. (D) In the validation set, $R^2Y = 0.8$ and $Q^2 = 0.774$. (E,F) Cluster analysis results in the discovery and validation sets, respectively. Intensities of metabolites used here were normalized to [0,1]. (G,H) RGB figure clearly discriminate the two groups in the discovery set and validation set, respectively. The samples from healthy volunteers are shown in "blue", whereas those from the early LC group are shown in "green".

protein digestion or protein catabolism; its downregulation may be related to the protein malnutrition of cancer reported in the literature.[10] Phenylglyoxylic acid belongs to the class of organic compounds known as benzoyl derivatives. The decreased levels of phenylglyoxylic acid may be a consequence of the reported downregulation of benzoic acid.[14] *N*-acetyltaurine is formed by the acetylation of taurine; its reduction may be related to the downregulation of taurine reported in the serum studies.[35] Acetyl-L-glutamic acid is deeply involved in the metabolism of glutamate and its significant downregulation was observed in the present study. Besides, a metabolic pathway map further verified the perturbations of biomarker candidates and correlated these feature metabolites to the disturbed metabolic pathways in the early LC group (Figure 3). The relevant metabolic pathway of the potential differential metabolites in early LC patients is provided in Table S4 Supporting Information.

Globally Disturbed Metabolic Pathways in the LC Group

To investigate the globally disturbed metabolic pathways in early LC patients, pathway analysis was completed based on the verified differential metabolites using MetaboAnalyst. As depicted in Figure 4A, the significant disorders of the amino acid metabolism were observed in the early LC group, including arginine and proline metabolism, arginine biosynthesis, valine, leucine and isoleucine biosynthesis, and so on. Moreover, the nucleotide metabolism was uncovered to be significantly disturbed including purine metabolism and aminoacyl-tRNA biosynthesis. It has been convinced that the active energy and purine metabolism sustained the uncontrolled growth of tumor cells.[36,37] The abnormal levels of purine compounds indicated metabolic disorders for a high proliferation rate of cancer cells, which was consistent with previous studies.[12,13] The significant change in the aminoacyl

https://doi.org/10.1021/acs.jproteome.1c00310
J. Proteome Res. 2021, 20, 4346−4356

transfer RNA biosynthesis pathway hinted at the dysregulation in mRNA translation for protein synthesis.[6,38]

To discover the molecular mechanisms during LC pathogenesis, RNASeq data of 35 patients diagnosed with LC and 35 nontumor adjacent normal lung tissues were obtained from the publicly available database. As expected, the transcriptome obviously segregated LC samples and other normal samples and the volcano plot indicated that 16,572 upregulated genes and 2853 downregulated genes were differentially expressed in the LC group, suggesting that there exists a dramatic molecular change during LC pathogenesis (Figure S8). Next, we further conducted the KEGG functional enrichment analysis to investigate the function of differentially expressed genes correlated with the LC (Figure 4B). The results displayed that among many other altered pathways, the amino acid metabolism was also affected such as protein digestion and absorption, tyrosine metabolism, biosynthesis of amino acids, arginine and proline metabolism, alanine, aspartate, and glutamate metabolism, glycine, serine, and threonine metabolism. Intriguingly, the disturbed biosynthesis of amino acids and amino acid metabolism observed in transcriptomics have been reflected in salivary metabolomics in this study. Additionally, these genes were also found to be enriched in salivary secretion, which confirms the importance and prospectiveness of saliva diagnosis in LC prediction. Furthermore, a heatmap was performed based on the differential genes evolved in metabolic pathways discussed above, clear separate clusters indicated that LC tissues can be well distinguished from controls (Figure 4C). The bar plot of disturbed metabolic pathways related to the LC phenotype based on KEGG pathway analysis is provided in Figure S9A, indicating the upregulation of the amino acid metabolism. What is more, top significant pathways in BP, CC, and MF of gene ontology analysis are shown in the bubble plot (Figure S9B).

Multivariate Analysis for Discrimination between Early LC Patients and Control Individuals

As shown in Figures S10−S13, 23 metabolites that are significantly differential in the early LC were defined as potential biomarkers and then evaluated by receiver operating characteristic (ROC) curves in the discovery and validation sets. In order to demonstrate the feasibility of this platform in early LC diagnosis, a panel consisting of these differential metabolites was established and applied for subsequent discriminant analysis. As shown in Figure 5A−D, early LC patients and healthy controls can be successfully discriminated in both discovery and validation sets for unsupervised PCA or supervised OPLS-DA. Cluster analysis was also employed to evaluate the diagnostic performance, and the cluster tree indicates that saliva samples from two groups appear in separate clusters with only one exception (healthy volunteer no. 5 was misclassified as an early LC patient) in the discovery set and two exceptions (healthy volunteer no. 23 was misclassified as an early LC patient and early LC patient no. 61 was misclassified as healthy control) in the validation set, respectively (Figure 5E,F). Besides, the digital red green blue (RGB) color map was created using three significant peaks. The color was composed by normalized R (m/z 134.0665), G (m/z 153.0178), and B (m/z 221.1198) values of each individual using MATLAB software. It suggests that the one shown in "blue" may be healthy, whereas the one shown in "green" has a high chance of being an early LC patient; this phenomenon can be observed in both the discovery set and the verification set (Figure 5G,H). The visual RGB figure helps us directly observe the disease information hidden in saliva samples, which could be conveniently used for the presentation of the disease diagnosis results in population screening.

Diagnosis of Early LC with the ANN Model

The 23 feature peaks were further set as the input layer of artificial neural networks to generate a prediction model, which was further validated to estimate the error rates using the normalized data collected from the verification cohort. As shown in Figure 6, the area under the ROC curve (AUC) of

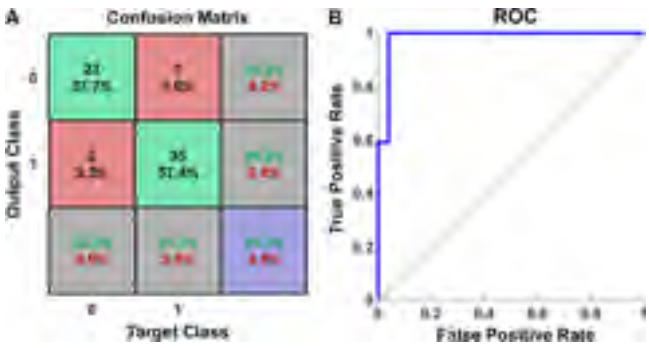

Figure 6. ANN model with prediction capability for early LC diagnosis. (A) Confusion matrix of the built prediction model using the normalized data collected from the verification cohort. (B) ROC curve of the potential biomarker panel for early LC diagnosis in the validation set.

the potential biomarker panel was 0.986 for early LC diagnosis in the validation set. The sensitivity and specificity of the prediction model in the verification cohort were 97.2 and 92%, respectively (Figure 6). The training parameters of the built model are provided in the Supporting Information (Figure S14). Furthermore, the potential biomarker panel was also applied to distinguish patients with advanced-stage LC from healthy controls or early LC patients. With the established model, advanced LC patients can be successfully separated from healthy controls with only one exception (Figure S15, Supporting Information). Also, the three groups can be successfully discriminated under supervised OPLS-DA (Figure S16, Supporting Information). With the well-trained ANN model, we envisioned that this TELDI-MS platform might return automatic, real-time results of diagnosis. In addition, we estimated the consumed time to complete a whole workflow using a batch of samples containing 96 saliva cases. The workflow includes sample preparation, TELDI MS data acquisition, and metabolic analysis. Because two steps of centrifugation are required to remove insoluble residues and precipitate proteins in saliva samples, the whole pretreatment process for the batch of samples takes 30 min. In TELDI-MS analysis, raw MS data of the batch of samples can be collected within 5 min with the automatic mode (Figure S17A, Supporting Information). Next, the raw spectrum of each saliva sample was converted into a .txt file within a few seconds. A self-written MATLAB script was utilized to immediately read the mass peaks of all saliva samples. After importing all mass peaks into R software, normalized metabolic features were extracted and further put into the established ANN model to provide nearly real-time prediction (Figure S17B, Supporting Information). As a result, the entire process

https://doi.org/10.1021/acs.jproteome.1c00310
J. Proteome Res. 2021, 20, 4346−4356

from sample preparation to the final diagnosis can be achieved within 50 min for a batch of samples containing 96 cases (Figure S17C, Supporting Information). These results gave us confidence that the established model based on the ultralow noise TELDI-MS platform has satisfactory diagnostic performance for clinical early screening of LC.

Possible Future Relevance for Clinical Practice

With the aid of the ultralow noise TELDI-MS platform, metabolic fingerprints of saliva samples were obtained in seconds using the FEP@VSiNW substrate, which showed great potentials in large-scale disease screening. The results of salivary metabolic analysis could potentially provide valuable complementary information for distinguishing early LC patients from healthy controls. Noninvasive sampling procedure, high sensitivity and specificity combined with rapid detection, and analysis in high throughput make the established platform possible for early screening of LC among the population, which may make some contributions to the improvement of overall survival. In the future, further possible applications might include mass screening of high-risk population such as heavy smokers. Besides, this salivary metabolic analysis platform might be suitable for screening of many other diseases such as various tumors, the metabolic fluctuations of which have been discovered in saliva samples.[6−8] More importantly, salivary metabolomics may provide a new insight for the diagnosis and prognosis of COVID-19, which is an emergent, worldwide public health concern during the pandemic.[39,40] Several works have confirmed the metabolic fluctuations in COVID-19 patients based on plasma or serum samples.[41−43] By analyzing the salivary metabolite profiles of COVID-19 patients at different disease progression stages, potential metabolic markers related to the phenotype may be discovered to help predict disease progression, recovery, and the therapeutic effects of clinical treatments.[40,44] Therefore, TELDI-MS, as a high-throughput salivary metabolite profiling platform, holds potentials in shedding light on finding disturbed metabolic pathways in COVID-19 patients and sorting out metabolic biomarkers with the clinical diagnostic value.

CONCLUSIONS

Overall, we demonstrated that an effective and rapid platform for salivary metabolic analysis using the FEP@VSiNW chip can be successfully applied to the noninvasive early diagnosis of LC. To minimize the external factors for salivary metabolomics, a total of six normalization techniques were investigated and compared in the metabolic analysis of saliva samples. Together with the good recognition of the salivary metabolic profiling for early LC patients, analysis of transcriptomic data from the online TCGA repository further verified the phenomenon found in salivary metabolomics that the metabolic status of early LC patients was significantly disturbed. The significantly differential metabolites were globally depicted, and a prediction model was built and verified for the early LC diagnosis with satisfactory discrimination performance. Overall, the high throughput MS platform for salivary metabolite profiling opened up a new possibility for early screening of LC.

ASSOCIATED CONTENT

Supporting Information

The Supporting Information is available free of charge at https://pubs.acs.org/doi/10.1021/acs.jproteome.1c00310.

Detailed procedure of saliva collection and preparation; experimental parameters of UPLC-MS analysis; R-scripts for data normalization; workflow of the statistical analysis of saliva samples; representative LDI mass spectra of saliva samples; box plots of peak ratio distributions obtained within the same batch of FEP@VSiNW substrates; box plots of peak ratio distribution obtained between different batches of substrates; variations within each metabolite between saliva samples from the HC group; variations within each metabolite between saliva samples from the early LC group; LDI mass spectra of saliva samples collected from HC and early LC patients in the metabolic fingerprint region; volcano plot showing the differential expressed genes between LC tissues and adjacent normal tissues; gene ontology and KEGG pathway enrichment analysis of differential genes; box plots of the normalized intensities of differential metabolites in the discovery set; box plots of the normalized intensities of differential metabolites in the validation set; ROC curves of the differential metabolites for early LC diagnosis in the discovery set; ROC curves of the differential metabolites for early LC diagnosis in the validation set; training parameters of the built prediction model for early LC diagnosis; confusion matrix and ROC curves of the built prediction model for advanced LC diagnosis; score plots for the OPLSDA model built with the selected metabolites; pipeline of nearly real-time molecular diagnosis of early LC by the TELDI-MS platform using the established ANN model; summary of feature peaks that could be used to distinguish early LC patients from control subjects; LC−MS/MS identification of potential feature peaks; MALDI-TOF/TOF MS/MS identification of salivary metabolites with commercial standard reagents; and metabolic pathway of the potential differential metabolites in early LC patients (PDF)

AUTHOR INFORMATION

Corresponding Authors

Haizhou Lou − *Department of Medical Oncology, Sir Run Run Shaw Hospital, School of Medicine, Zhejiang University, Hangzhou 310016, China*; Email: louhz09@zju.edu.cn

Jianmin Wu − *Institution of Analytical Chemistry, Department of Chemistry, Zhejiang University, Hangzhou 310058, China*; orcid.org/0000-0002-0999-9194; Email: wjmst1@zju.edu.cn

Authors

Xinrong Jiang − *Institution of Analytical Chemistry, Department of Chemistry, Zhejiang University, Hangzhou 310058, China*

Xiaoming Chen − *Institution of Analytical Chemistry, Department of Chemistry, Zhejiang University, Hangzhou 310058, China; Well-Healthcare Technologies Co., Hangzhou 310051, China*

https://doi.org/10.1021/acs.jproteome.1c00310
J. Proteome Res. 2021, 20, 4346−4356

Zhao Chen − *Department of Thoracic Surgery, Sir Run Run Shaw Hospital, School of Medicine, Zhejiang University, Hangzhou 310016, China*

Jiekai Yu − *Institute of Cancer Research, The Second Affiliated Hospital of Zhejiang University, Hangzhou 310009, China*

Complete contact information is available at: https://pubs.acs.org/10.1021/acs.jproteome.1c00310

Author Contributions

All authors have given approval to the final version of the manuscript.

Funding

This study is supported by grants from the National Natural Science Foundation of China [grants number 21874118 and 21575127].

Notes

The authors declare no competing financial interest.

Ethics approval and consent to participate. Saliva samples were obtained from Sir Run Run Shaw Hospital of Zhejiang University. The Ethical Committee of the Sir Run Run Shaw Hospital of Zhejiang University approved the protocol (no. 20201028-39), and the study was performed in accordance with the ethical standards laid down in the 1964 Declaration of Helsinki and its later amendments. Written informed consent from each patient was achieved. The data that support the findings of this study are available from the corresponding author upon reasonable request.

■ ACKNOWLEDGMENTS

We thank the strong support of Sir Run Run Shaw Hospital for the saliva sample collection project and the contributions of all volunteers who participated in the collection project.

■ ABBREVIATIONS

FC, fold change; KEGG, Kyoto Encyclopedia of Genes and Genomes; BP, biological process; MF, molecular function; CC, cellular component

■ REFERENCES

(1) Sung, H.; Ferlay, J.; Siegel, R. L.; Laversanne, M.; Soerjomataram, I.; Jemal, A.; Bray, F. Global Cancer Statistics 2020: GLOBOCAN Estimates of Incidence and Mortality Worldwide for 36 Cancers in 185 Countries. *CA A Cancer J. Clin.* **2021**, *71*, 209−249.

(2) Barros, J. A.; Valladares, G.; Faria, A. R.; Fugita, E. M.; Ruiz, A. P.; Vianna, A. G. D.; Trevisan, G. L.; de Oliveira, F. A. M. Early diagnosis of lung cancer: the great challenge. Epidemiological variables, clinical variables, staging and treatment. *J. Bras. Pneumol.* **2006**, *32*, 221−227.

(3) Pirozynski, M. Retraction Notice to ″100 years of lung cancer″ [Respiratory Medicine 100(12) (2006) 2073-2084]. *Respir. Med.* **2009**, *103*, 1244.

(4) Aberle, D. R.; Adams, A. M.; Berg, C. D.; Black, W. C.; Clapp, J. D.; Fagerstrom, R. M.; Gareen, I. F.; Gatsonis, C.; Marcus, P. M.; Sicks, J. D. Reduced lung-cancer mortality with low-dose computed tomographic screening. *N. Engl. J. Med.* **2011**, *365*, 395−409.

(5) de Almeida Pdel, P.; Gregio, A. M.; Machado, M. A.; de Lima, A. A.; Azevedo, L. R. Saliva composition and functions: a comprehensive review. *J. Contemp. Dent. Pract.* **2008**, *9*, 72−80.

(6) Song, X.; Yang, X.; Narayanan, R.; Shankar, V.; Ethiraj, S.; Wang, X.; Duan, N.; Ni, Y.-H.; Hu, Q.; Zare, R. N. Oral squamous cell carcinoma diagnosed from saliva metabolic profiling. *Proc. Natl. Acad. Sci. U. S. A.* **2020**, *117*, 16167−16173.

(7) Zhong, L.; Cheng, F.; Lu, X.; Duan, Y.; Wang, X. Untargeted saliva metabonomics study of breast cancer based on ultra performance liquid chromatography coupled to mass spectrometry with HILIC and RPLC separations. *Talanta* **2016**, *158*, 351−360.

(8) Grimaldi, M.; Palisi, A.; Rossi, G.; Stillitano, I.; Faiella, F.; Montoro, P.; Rodriquez, M.; Palladino, R.; Maria D'Ursi, A.; Romano, R. Saliva of patients affected by salivary gland tumour: An NMR metabolomics analysis. *J. Pharm. Biomed. Anal.* **2018**, *160*, 436−442.

(9) Tang, Y.; Li, Z.; Lazar, L.; Fang, Z.; Tang, C.; Zhao, J. Metabolomics workflow for lung cancer: Discovery of biomarkers. *Clin. Chim. Acta* **2019**, *495*, 436−445.

(10) Callejón-Leblic, B.; García-Barrera, T.; Grávalos-Guzmán, J.; Pereira-Vega, A.; Gómez-Ariza, J. L. Metabolic profiling of potential lung cancer biomarkers using bronchoalveolar lavage fluid and the integrated direct infusion/ gas chromatography mass spectrometry platform. *J. Proteomics* **2016**, *145*, 197−206.

(11) Pamungkas, A. D.; Park, C.; Lee, S.; Jee, S. H.; Park, Y. H. High resolution metabolomics to discriminate compounds in serum of male lung cancer patients in South Korea. *Respir. Res.* **2016**, *17*, 100.

(12) You, L.; Fan, Y.; Liu, X.; Shao, S.; Guo, L.; Noreldeen, H. A. A.; Li, Z.; Ouyang, Y.; Li, E.; Pan, X.; Liu, T.; Tian, X.; Ye, F.; Li, X.; Xu, G. Liquid Chromatography-Mass Spectrometry-Based Tissue Metabolic Profiling Reveals Major Metabolic Pathway Alterations and Potential Biomarkers of Lung Cancer. *J. Proteome Res.* **2020**, *19*, 3750−3760.

(13) Moreno, P.; Jiménez-Jiménez, C.; Garrido-Rodríguez, M.; Calderón-Santiago, M.; Molina, S.; Lara-Chica, M.; Priego-Capote, F.; Salvatierra, Á.; Muñoz, E.; Calzado, M. A. Metabolomic profiling of human lung tumor tissues - nucleotide metabolism as a candidate for therapeutic interventions and biomarkers. *Mol. Oncol.* **2018**, *12*, 1778−1796.

(14) Mu, Y.; Zhou, Y.; Wang, Y.; Li, W.; Zhou, L.; Lu, X.; Gao, P.; Gao, M.; Zhao, Y.; Wang, Q.; Wang, Y.; Xu, G. Serum Metabolomics Study of Nonsmoking Female Patients with Non-Small Cell Lung Cancer Using Gas Chromatography-Mass Spectrometry. *J. Proteome Res.* **2019**, *18*, 2175−2184.

(15) Chen, W.; Lu, S.; Ou, J.; Wang, G.; Zu, Y.; Chen, F.; Bai, C. Metabonomic characteristics and biomarker research of human lung cancer tissues by HR1H NMR spectroscopy. *Canc. Biomarkers* **2016**, *16*, 653−664.

(16) Mueller, D. C.; Piller, M.; Niessner, R.; Scherer, M.; Scherer, G. Untargeted metabolomic profiling in saliva of smokers and non-smokers by a validated GC-TOF-MS method. *J. Proteome Res.* **2014**, *13*, 1602−1613.

(17) Merlos Rodrigo, M. A.; Zitka, O.; Krizkova, S.; Moulick, A.; Adam, V.; Kizek, R. MALDI-TOF MS as evolving cancer diagnostic tool: a review. *J. Pharm. Biomed. Anal.* **2014**, *95*, 245−255.

(18) Fuchs, B.; Süß, R.; Schiller, J. An update of MALDI-TOF mass spectrometry in lipid research. *Prog. Lipid Res.* **2011**, *50*, 132.

(19) Trim, P. J.; Snel, M. F. Small molecule MALDI MS imaging: Current technologies and future challenges. *Methods* **2016**, *104*, 127−141.

(20) Jiang, X.; Chen, X.; Wang, T.; Li, Y.; Pan, A.; Wu, J. Perfluorinated polymer modified vertical silicon nanowires as ultra low noise laser desorption ionization substrate for salivary metabolites profiling. *Talanta* **2021**, *225*, 122022.

(21) Chen, X.; Wang, T.; Lin, L.; Wo, F.; Liu, Y.; Liang, X.; Ye, H.; Wu, J. Tip-Enhanced Photoinduced Electron Transfer and Ionization on Vertical Silicon Nanowires. *ACS Appl. Mater. Interfaces* **2018**, *10*, 14389−14398.

(22) Bellagambi, F. G.; Lomonaco, T.; Salvo, P.; Vivaldi, F.; Hangouët, M.; Ghimenti, S.; Biagini, D.; Di Francesco, F.; Fuoco, R.; Errachid, A. Saliva sampling: Methods and devices. An overview. *Trac. Trends Anal. Chem.* **2020**, *124*, 115781.

(23) Vogl, F. C.; Mehrl, S.; Heizinger, L.; Schlecht, I.; Zacharias, H. U.; Ellmann, L.; Nürnberger, N.; Gronwald, W.; Leitzmann, M. F.; Rossert, J.; Eckardt, K.-U.; Dettmer, K.; Oefner, P. J. Evaluation of dilution and normalization strategies to correct for urinary output in

HPLC-HRTOFMS metabolomics. *Anal. Bioanal. Chem.* **2016**, *408*, 8483−8493.
(24) Ejigu, B. A.; Valkenborg, D.; Baggerman, G.; Vanaerschot, M.; Witters, E.; Dujardin, J.-C.; Burzykowski, T.; Berg, M. Evaluation of normalization methods to pave the way towards large-scale LC-MS-based metabolomics profiling experiments. *OMICS* **2013**, *17*, 473−485.
(25) Wu, Y.; Li, L. Sample normalization methods in quantitative metabolomics. *J. Chromatogr. A* **2016**, *1430*, 80−95.
(26) Warrack, B. M.; Hnatyshyn, S.; Ott, K.-H.; Reily, M. D.; Sanders, M.; Zhang, H.; Drexler, D. M. Normalization strategies for metabonomic analysis of urine samples. *J. Chromatogr. B: Anal. Technol. Biomed. Life Sci.* **2009**, *877*, 547−552.
(27) Cook, T.; Ma, Y.; Gamagedara, S. Evaluation of statistical techniques to normalize mass spectrometry-based urinary metabolomics data. *J. Pharm. Biomed. Anal.* **2020**, *177*, 112854.
(28) Khamis, M. M.; Holt, T.; Awad, H.; El-Aneed, A.; Adamko, D. J. Comparative analysis of creatinine and osmolality as urine normalization strategies in targeted metabolomics for the differential diagnosis of asthma and COPD. *Metabolomics* **2018**, *14*, 115.
(29) Wen, T.; Gao, L.; Wen, Z.; Wu, C.; Tan, C. S.; Toh, W. Z.; Ong, C. N. Exploratory investigation of plasma metabolomics in human lung adenocarcinoma. *Mol. Biosyst.* **2013**, *9*, 2370−2378.
(30) Kim, H. J.; Jang, S. H.; Ryu, J.-S.; Lee, J. E.; Kim, Y. C.; Lee, M. K.; Jang, T. W.; Lee, S.-Y.; Nakamura, H.; Nishikata, N.; Mori, M.; Noguchi, Y.; Miyano, H.; Lee, K. Y. The performance of a novel amino acid multivariate index for detecting lung cancer: A case control study in Korea. *Lung Cancer* **2015**, *90*, 522−527.
(31) Maeda, J.; Higashiyama, M.; Imaizumi, A.; Nakayama, T.; Yamamoto, H.; Daimon, T.; Yamakado, M.; Imamura, F.; Kodama, K. Possibility of multivariate function composed of plasma amino acid profiles as a novel screening index for non-small cell lung cancer: a case control study. *BMC Canc.* **2010**, *10*, 690.
(32) Hori, S.; Nishiumi, S.; Kobayashi, K.; Shinohara, M.; Hatakeyama, Y.; Kotani, Y.; Hatano, N.; Maniwa, Y.; Nishio, W.; Bamba, T.; Fukusaki, E.; Azuma, T.; Takenawa, T.; Nishimura, Y.; Yoshida, M. A metabolomic approach to lung cancer. *Lung Canc.* **2011**, *74*, 284−292.
(33) Wikoff, W. R.; Grapov, D.; Fahrmann, J. F.; DeFelice, B.; Rom, W. N.; Pass, H. I.; Kim, K.; Nguyen, U.; Taylor, S. L.; Gandara, D. R.; Kelly, K.; Fiehn, O.; Miyamoto, S. Metabolomic markers of altered nucleotide metabolism in early stage adenocarcinoma. *Canc. Prev. Res.* **2015**, *8*, 410−418.
(34) Carrola, J.; Rocha, C. M.; Barros, A. S.; Gil, A. M.; Goodfellow, B. J.; Carreira, I. M.; Bernardo, J.; Gomes, A.; Sousa, V.; Carvalho, L.; Duarte, I. F. Metabolic signatures of lung cancer in biofluids: NMR-based metabonomics of urine. *J. Proteome Res.* **2011**, *10*, 221−230.
(35) Li, Y.-Q.; Liu, Y.-F.; Song, D.-D.; Zhou, Y.-P.; Wang, L.; Xu, S.; Cui, Y.-F. Particle swarm optimization-based protocol for partial least-squares discriminant analysis: Application to 1H nuclear magnetic resonance analysis of lung cancer metabonomics. *Chemom. Intell. Lab. Syst.* **2014**, *135*, 192−200.
(36) Pavlova, N. N.; Thompson, C. B. The Emerging Hallmarks of Cancer Metabolism. *Cell Metabol.* **2016**, *23*, 27−47.
(37) Spychala, J. Tumor-promoting functions of adenosine. *Pharmacol. Ther.* **2000**, *87*, 161−173.
(38) Kim, S.; You, S.; Hwang, D. Aminoacyl-tRNA synthetases and tumorigenesis: more than housekeeping. *Nat. Rev. Canc.* **2011**, *11*, 708−718.
(39) Zhu, N.; Zhang, D.; Wang, W.; Li, X.; Yang, B.; Song, J.; Zhao, X.; Huang, B.; Shi, W.; Lu, R.; Niu, P.; Zhan, F.; Ma, X.; Wang, D.; Xu, W.; Wu, G.; Gao, G. F.; Tan, W. A Novel Coronavirus from Patients with Pneumonia in China, 2019. *N. Engl. J. Med.* **2020**, *382*, 727−733.
(40) Costa dos Santos Junior, G.; Pereira, C. M.; Kelly da Silva Fidalgo, T.; Valente, A. P. Saliva NMR-Based Metabolomics in the War Against COVID-19. *Anal. Chem.* **2020**, *92*, 15688−15692.
(41) Shen, B.; Yi, X.; Sun, Y.; Bi, X.; Du, J.; Zhang, C.; Quan, S.; Zhang, F.; Sun, R.; Qian, L.; Ge, W.; Liu, W.; Liang, S.; Chen, H.; Zhang, Y.; Li, J.; Xu, J.; He, Z.; Chen, B.; Wang, J.; Yan, H.; Zheng, Y.; Wang, D.; Zhu, J.; Kong, Z.; Kang, Z.; Liang, X.; Ding, X.; Ruan, G.; Xiang, N.; Cai, X.; Gao, H.; Li, L.; Li, S.; Xiao, Q.; Lu, T.; Zhu, Y.; Liu, H.; Chen, H.; Guo, T. Proteomic and Metabolomic Characterization of COVID-19 Patient Sera. *Cell* **2020**, *182*, 59−72.
(42) Delafiori, J.; Navarro, L. C.; Siciliano, R. F.; de Melo, G. C.; Nicolau, J. C.; Sales, G. M.; de Oliveira, A. N.; Val, F. F. A.; de Oliveira, D. N.; Eguti, A.; dos Santos, L. A.; Dalçóquio, T. F.; Bertolin, A. J.; Abreu-Netto, R. L.; Salsoso, R.; Baía-da-Silva, D.; Marcondes-Braga, F. G.; Sampaio, V. S.; Judice, C. C.; Costa, F. T. M.; Durán, N.; Perroud, M. W.; Sabino, E. C.; Lacerda, M. V. G.; Reis, L. O.; Fávaro, W. J.; Monteiro, W. M.; Rocha, A. R.; Catharino, R. R.; Catharino, R. R. Covid-19 Automated Diagnosis and Risk Assessment through Metabolomics and Machine Learning. *Anal. Chem.* **2021**, *93*, 2471−2479.
(43) Kimhofer, T.; Lodge, S.; Whiley, L.; Gray, N.; Loo, R. L.; Lawler, N. G.; Nitschke, P.; Bong, S.-H.; Morrison, D. L.; Begum, S.; Richards, T.; Yeap, B. B.; Smith, C.; Smith, K. G. C.; Holmes, E.; Nicholson, J. K. Integrative Modeling of Quantitative Plasma Lipoprotein, Metabolic, and Amino Acid Data Reveals a Multiorgan Pathological Signature of SARS-CoV-2 Infection. *J. Proteome Res.* **2020**, *19*, 4442−4454.
(44) Mahmud, I.; Garrett, T. J. Mass Spectrometry Techniques in Emerging Pathogens Studies: COVID-19 Perspectives. *J. Am. Soc. Mass Spectrom.* **2020**, *31*, 2013−2024.

https://doi.org/10.1021/acs.jproteome.1c00310
J. Proteome Res. 2021, 20, 4346−4356